Purdue University
Purdue e-Pubs

Birck and NCN Publications

Birck Nanotechnology Center

2-26-2007

Valley splitting in strained silicon quantum wells modeled with 2 degrees miscuts, step disorder, and alloy disorder

Neerav Kharche
Birck Nanotechnology Center and Purdue University, nkharche@purdue.edu

Marta Prada
School of Electrical and Computer Engineering, Purdue University, mprada@purdue.edu

Timothy Boykin
Department of Electrical and Computer Engineering, University of Alabama

Gerhard Klimeck
Purdue University, gekco@purdue.edu

Follow this and additional works at: http://docs.lib.purdue.edu/nanopub

Valley splitting in strained silicon quantum wells modeled with 2° miscuts, step disorder, and alloy disorder

Neerav Kharche[a)] and Marta Prada
*School of Electrical and Computer Engineering, Purdue University, West Lafayette, Indiana 47907 and
Network for Computational Nanotechnology, Purdue University, West Lafayette, Indiana 47907*

Timothy B. Boykin
Department of Electrical and Computer Engineering, University of Alabama, Huntsville, Alabama 35899

Gerhard Klimeck
*School of Electrical and Computer Engineering, Purdue University, West Lafayette, Indiana 47907;
Network for Computational Nanotechnology, Purdue University, West Lafayette, Indiana 47907; and Jet
Propulsion Laboratory, Caltech, Pasadena, California 91109*

Valley splitting (VS) in strained SiGe/Si/SiGe quantum wells grown on (001) and 2° miscut substrates is computed in a magnetic field. Calculations of flat structures significantly overestimate, while calculations of perfectly ordered structures underestimate experimentally observed VS. Step disorder and confinement alloy disorder raise the VS to the experimentally observed levels. Atomistic alloy disorder is identified as the critical physics, which cannot be modeled with analytical effective mass theory. NEMO-3D is used to simulate up to 10^6 atoms, where strain is computed in the valence-force field and electronic structure in the $sp^3d^5s^*$ model. © *2007 American Institute of Physics.* [DOI: 10.1063/1.2591432]

Silicon based quantum computing (QC) architectures[1–3] are pursued[4,5] due to their potential for scaling and their expected long decoherence times.[6] However, the presence of valley degeneracy in the conduction band of Si is often perceived as a problem for QC, leading to decoherence.[7] Biaxial strain separates the sixfold degeneracy into a lower twofold and a raised fourfold degeneracy. Symmetry breaking due to quantum confinement can further[8] split the twofold degeneracy, called valley splitting (VS). Each VS state is spin split by a magnetic field and the relative size of the splittings needs to be designed carefully for realistic qubits.

Experimental evidence shows that the VS is overpredicted by at least one order of magnitude when a flat ideal quantum well (QW) is assumed.[9] This overprediction has been associated with the experimental condition that the QWs are typically grown on a 2° tilted [001] substrate. Treatments in small atomistic representations support this claim.[10] Effective mass treatments[12,11] can explain the behavior of VS in miscut QWs; however, they rely on perturbation theories and *ad hoc* structure dependent fitting parameters and they cannot address the atomistic alloy disorder at the interface. This work expands on these concepts, represents strain and interfaces atomistically, and includes disorder at the steps[13] and disorder in the confining alloy, without any *ad hoc* fitting parameters. The general purpose code NEMO-3D Ref. 14 is utilized to perform multimillion atom simulations in domains that are large enough to be representative of realistic device geometries.

The physics of VS in a flat [001] QW where four propagating states ($\pm k_z^1, \pm k_z^2$) form two bound states is discussed in detail in Ref. 8. The VS physics of the miscut QW is significantly different. The detailed atomistic view of the unit cell of a miscut QW grown on a $[\bar{1}0n]$ substrate is shown in the

xz plane in Fig. 1(a). The origin of VS in an ideal miscut QW is explained pictorially in Figs. 1(b)–1(d). In an analytical view where m_t and m_l are the bulk Si transverse and longitudinal effective masses, the effective mass of the projected *z* valleys along the [*n*01] direction is $1/m_{\rm eff} = \cos^2(\theta_T)/m_t$
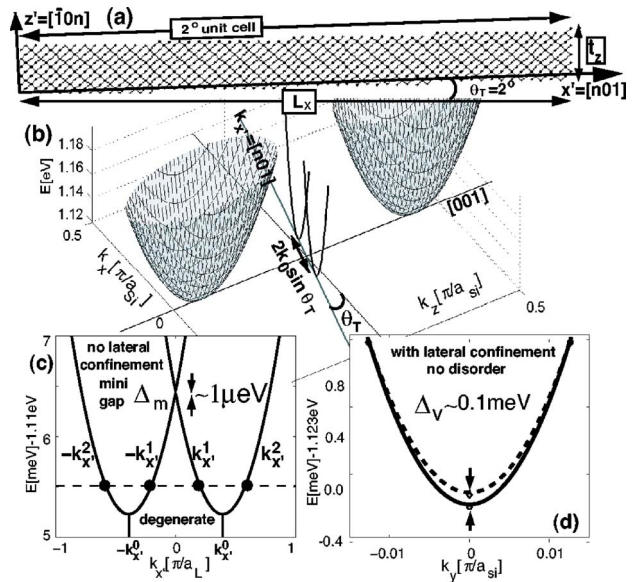

FIG. 1. (Color online) VS in an ideal miscut QW: (a) minimal ideal unit cell of a miscut QW consisting of four steps ($n=28$ for 2° tilt). (b) Band structure of a miscut QW grown on the *z′* surface can be obtained by projecting conduction band valleys at $(0,0,\pm k_0)$ onto the QW growth surface Ref. 19. Two degenerate valleys are located at $k_{x'}^0 = \pm k_0 \sin(\theta_T)$ along [*n*01]. (c) Valley-valley interaction at the crossing causes a minigap (Δ_m) at Γ Refs. 20 and 21. Lowest valleys are degenerate. Here, $a_L = na_{\rm Si}$. (d) Confinement the in *x′* direction causes quadrate of states in two degenerate valleys centered at $k_{x'} = \pm k_{x'}^0$ to interact and split. All band structures in (b)–(d) are calculated with $sp^3d^5s^*$ with spin-orbit coupling. Conventional tetrahedral unit cell is used to obtain bulk Si band structures of (b). Lateral extensions of QWs of (c) and (d) are $L_x=15.33$ nm, $L_y=0.55$ nm, and thickness is $t_z=5.26$ nm.

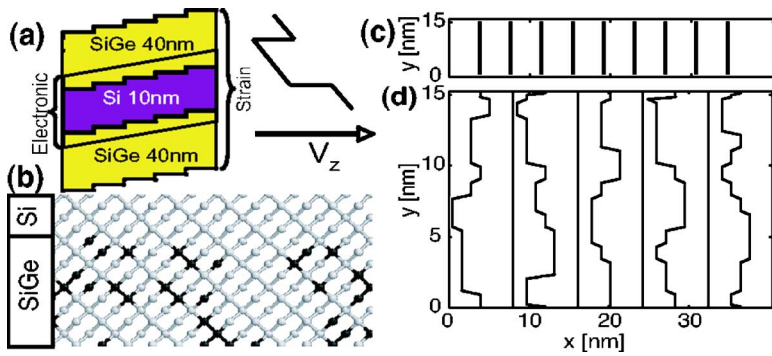[a)]Electronic mail: nkharche@purdue.edu

FIG. 2. (Color online) (a) Schematic of SiGe/Si/SiGe heterostructure and confining potential (V_z) along growth direction. (b) Atomic scale representation of a disordered Si/SiGe interface. (c) Ideal steps along the [100] direction in the xy plane. (d) Schematic of the step disorder along the y direction in Si/SiGe heterostructures grown on 2° miscut substrates. Flat and disordered steps alternate Ref. 13.

$+\sin^2(\theta_T)/m_l$, which is in agreement with our tight-binding calculations. Here, the tilt angle $\theta_T=\tan^{-1}(1/n)$ is the angle between the [100] and [n01] crystal directions. At Γ a small minigap forms similar to the flat QW case. This gap is, however, significantly higher in energy than the two degenerate valleys at $\pm k_{x'}^0$. Additional lateral confinement is needed in miscut QWs to split the degeneracy of these lowest valleys which can be provided by lateral electrostatic gates or a magnetic field.[9,10]

The $Si_{1-x}Ge_x$/Si/SiGe ($x=0.30$) structure proposed in the architecture in Refs. 5 and 11 is fabricated on miscut QWs sketched in Fig. 2(a). Modulation doping induces a two-dimensional electron gas (2DEG) associated with a built-in electrostatic potential. Figure 2(b) shows a zoomed view of a possible random interface configuration when the SiGe buffer is represented explicitly. Slanted QWs can be assumed in a first approximation to be made up of repeated regular steps [Figs. 2(a) and 2(c)] creating a tilt angle (θ_T) to the [100] direction in the growth plane, causing the unit cell to be large compared to that of a flat QW. However, Si QWs grown on miscut substrates have an irregular steplike structure along the [100] crystallographic axis[13] [Fig. 2(d)]. The remaining part of the letter focuses on the description of various models used in simulation of realistic QWs and their effect on VS. VS in flat QWs is computed for comparison.

NEMO-3D represents each atom in the simulation domain explicitly. The Keating potential valence-force field model[15] is used to move the atoms to positions which minimize the total strain energy. A subsequent electronic structure calculation is based on the 20 band $sp^3d^5s^*$ tight-binding model. The strain is included in the tight-binding Hamiltonian.[14]

Modulation doping induces a built-in electric field [Fig. 2(a)]. Here we do not solve the electrostatic potential self-consistently but focus on the essential physics and assume a constant electric field of 9 MV/m along the growth direction.[9]

The magnetic field is included by using gauge-invariant Peierls substitution.[16] The spin contribution to the magnetic moment is included by adding $\mu_B \sigma \mathbf{B}$ to the diagonal matrix elements, where μ_B is Bohr magneton and σ are Pauli spin matrices.

Irregularities in the y direction along the steps [Fig. 2(d)] are implemented on the atomic scale using kink distributions based on step and kink energies from experimental data.[13] Step disorder is assumed to be quasiperiodic in the y direction, with a lateral extension of 15 nm. With periodicity in the y direction and a magnetic field in the z direction, a choice of the Landau gauge, $\mathbf{A}=Bx\hat{y}$ for the vector potential appears to be natural. However, due to the x-coordinate dependence of this gauge the device geometry cannot be taken

as periodic. The system must therefore be closed in the x direction, which will indeed introduce confinement effects. The artificial confinement induced by these spatial boundary conditions competes with the realistic magnetic confinement effects. The lateral x dimension is set to 150 nm, which is about seven times larger than the maximum magnetic confinement length in a 2DEG at $B=1.5$ T ($\simeq 21$ nm). For the magnetic field range of 1.5–4 T no lateral x-confinement effects due to the closed boundary conditions are visible in our simulations. Confinement is dominated by the magnetic field.

40 nm of SiGe layers are included on the top and the bottom of a 10 nm Si QW for strain calculations. This SiGe thickness is sufficient to model the long range strain disorder.[17] Since the electronic states of interest in this problem are spatially confined to the QW and only weakly penetrate into the SiGe, one can safely reduce the electronic structure domain to 3 nm of SiGe buffer around the Si QW. These computationally extensive simulations contain around (10 and 1.9)$\times 10^6$ atoms in the strain and electronic structure domains, respectively. The computations were performed on nanoHUB.org computational resources[18] requiring typically 20 CPUs for 30 h for each run. For the idealized geometries without a SiGe buffer, a homogeneous lattice distortion of $\epsilon_{\parallel}=0.013$ is assumed throughout the Si QW, as approximated from the full SiGe buffer system calculation and hard wall boundary conditions are assumed in the z direction. Here the electronic structure domain includes only 1.2×10^6 atoms. Typical calculations required 15 h on 20 CPUs.[18]

VS is larger than spin splitting (SS) [Fig. 3(a)] as desired for QC. Inclusion of realistically disordered, interfaces (atom
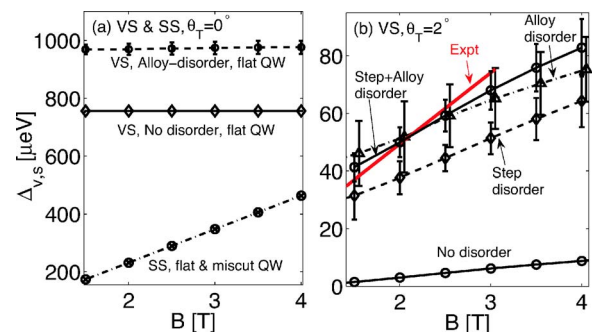

FIG. 3. (Color online) (a) VS in a flat QW and SS in flat and miscut QWs. VS increases due to the SiGe alloy disorder. SS remains unchanged by disorders or miscut surfaces. (b) VS in 2° miscut Si QWs in the presence of realistic disorders. Error bars represent standard deviation in VS. VS is enhanced due to step as well as alloy disorder and is on the same order of magnitude as reported in experiments Ref. 9.

disorder, position disorder, and inhomogeneous strain) raises VS further. Error bars represent the standard deviation in VS obtained from five different samples of random SiGe alloy disorder. Further statistical analysis is under way requiring significantly more computation time. However, we believe that the average values already predict the general physics. The presence of the high electric field in the QW makes VS virtually insensitive to small variations in thickness.[8] Therefore the enhancement of VS is solely the effect of alloy disorder and not the effective increase in QW thickness due to "softer" SiGe barriers. Atomistic numerical simulation is needed to address this physics.

VS in 2° miscut QWs is suppressed by at least two orders of magnitude as compared to flat QWs [Fig. 3(a) and 3(b)]. SS, however, is not affected by the disorder or the change in substrate orientation since it is a result of the geometry independent spin correction $\mu_B \sigma \mathbf{B}$. The Landé g factor extracted from the SS plots in Fig. 3(a) is 2.0028, which is very close to the ideal free-electron value as reported in Ref. 9. The computed VS in 2° miscut QWs [Fig. 3(b)] scales linearly with the magnetic field as observed in Ref. 9.

Realistic miscut QWs have two types of disorders: Alloy disorder (atom disorder, position disorder, and inhomogeneous strain) [Fig. 2(b)] and step disorder [Fig. 2(d)]. Figure 3(b) shows VS obtained from five different samples for each of random alloy disorder, step disorder and both disorders combined. Both disorders alone create significantly increased VS. Among these alloy disorder produces a rapidly varying spatial surface disorder. Figure 3(b) shows that slowly varying step disorder [Fig. 2(d)] alone does not raise VS to observed values. Alloy disorder alone can raise VS to experimentally observed values[9] dominating the effect of raised VS. High frequency alloy disorder plays the dominant role in the enhancement of VS in miscut QWs and not the parameter sensitive step disorder.[11] VS computed with both disorders [Fig. 3(b)] shows a linear behavior as observed in low field measurements.[9] Continuum effective mass theories[12,11] do not address the dependence of VS on alloy disorder and atomistic simulations as presented here are needed. VS that is smaller than SS leads to the loss of information outside spin-1/2 Quantum bit Hilbert space making them inadequate for spin-based QC. Recent experiments have achieved VS higher than SS in miscut QWs by electrostatic gating, which produces stronger confinement than magnetic fields.[9]

Using the powerful NEMO-3D tool, we are able to incorporate the effects of a miscut surface at atomic level in *realistic* SiGe/Si/SiGe QWs and observe a VS in accordance with the experimental results, where both step roughness and SiGe alloy disorders are included, enabling the prediction of VS in realistic experiments. Key findings of this work are as follows: (1) Lateral confinement is necessary to break the degeneracy of the lowest energy states in miscut QWs. (2) Disorder increases VS in miscut QWs by an order of magnitude but is not sufficient to raise it beyond SS as required for spin-based QC architectures. (3) A very high lateral confinement typically provided by electrostatic gates is necessary to raise VS above SS in miscut QWs. (4) While all calculations in this work are performed in atomistic tight binding, the flat and ordered miscut QW physics can be supported by an effective mass model. (5) Atomic details of alloy disorder and step disorder are critical for modeling VS, which cannot be addressed with continuum effective mass theory. (6) Alloy disorder in the confinement is a dominating effect over step disorder.

[1] B. E. Kane, Nature (London) **393**, 133 (1998).

[2] R. Vrijen, E. Yablonovitch, K. Wang, H. Jiang, A. Balandin, V. Roychowdhury, T. Mor, and D. DiVencenzo, Phys. Rev. A **62**, 012306 (2000).

[3] D. Loss and D. P. DiVincenzo, Phys. Rev. A **57**, 120 (1998).

[4] M. Friesen, P. Rugheimer, D. E. Savage, M. G. Lagally, D. van der Weide, R. Joynt, and M. A. Eriksson, Phys. Rev. B **67**, 121301 (2003).

[5] M. A. Eriksson, M. Friesen, S. N. Coppersmith, R. Joynt, L. J. Klein, K. Slinker, C. Tahan, P. M. Mooney, J. O. Chu, and S. J. Koester, Quantum Inf. Process. **3**, 133 (2004).

[6] C. Tahan, M. Friesen, and R. Joynt, Phys. Rev. B **66**, 035314 (2002).

[7] B. Koiller, X. D. Hu, and S. Das Sarma, Phys. Rev. Lett. **88**, 027903 (2002).

[8] T. B. Boykin, G. Klimeck, M. A. Eriksson, M. Friesen, S. N. Coppersmith, P. von Allmen, F. Oyafuso, and S. Lee, Appl. Phys. Lett. **84**, 115 (2004); T. B. Boykin, G. Klimeck, M. Friesen, S. N. Coppersmith, P. von Allmen, F. Oyafuso, and S. Lee, Phys. Rev. B **70**, 165325 (2004).

[9] S. Goswami, M. Friesen, J. L. Truitt, C. Tahan, L. J. Klein, J. O. Chu, P. M. Mooney, D. van der Weide, S. N. Coppersmith, R. Joynt, and M. A. Erikson, e-print cond-mat/0408389; S. Goswami, K. A. Slinker, Mark Friesen, L. M. McGuire, J. L. Truitt, Charles Tahan, L. J. Klein, J. O. Chu, P. M. Mooney, D. W. van der Weide, Robert Joynt, S. N. Coppersmith, and Mark A. Eriksson, e-print cond-mat/0611221.

[10] P. von Allmen and S. Lee, e-print cond-mat/0606395.

[11] M. Friesen, M. A. Eriksson, and S. N. Coppersmith, Appl. Phys. Lett. **89**, 202106 (2006); M. Friesen, S. Chutia, C. Tahan, and S. N. Coppersmith, e-print cond-mat/0608229.

[12] T. Ando, Phys. Rev. B **19**, 3089 (1979).

[13] H. J. W. Zandviet and H. B. Elswijk, Phys. Rev. B **48**, 14269 (1993).

[14] G. Klimeck, F. Oyafuso, T. B. Boykin, R. C. Bowen, and P. von Allmen, Comput. Model. Eng. Sci. **3**, 601 (2002).

[15] P. N. Keating, Phys. Rev. **145**, 637 (1966); **66**, 125207 (2002).

[16] T. B. Boykin, R. Chris Bowen, and Gerhard Klimeck, Phys. Rev. B **63**, 245314 (2001); M. Graf and P. Vogl, Phys. Rev. B **51**, 4940 (1995).

[17] M. Korkusinski, Gerhard Klimeck, Haiying Xu, Seungwon Lee, Sebastien Goasguen, and Faisal Saied, Proceedings of 2005 NSTI Conference, Anaheim, CA, 8–12 May 2005 (unpublished).

[18] Computational resource of a 256 node 3.3 GHz Pentium Irvindale PC cluster (nanoHUB.org).

[19] L. J. Sham, S. J. Allen, Jr., A. Kamgar, and D. C. Tsui, Phys. Rev. Lett. **40**, 472 (1978).

[20] J. B. Veiga Salles, H. Closs, J. R. Senna, and P. J. Stiles, Phys. Rev. B **37**, 8912 (1988).

[21] T. J. Thornton, F. Ge, A. Andresen, D. Pivin, J. Bird, and D. K. Ferry, J. Vac. Sci. Technol. B **17**, 1757 (1999).